

Magnetic properties of HITPERM (Fe,Co)₈₈Zr₇B₄Cu₁ magnets

M. A. Willard,^{a)} M.-Q. Huang, D. E. Laughlin, and M. E. McHenry
*Department of Materials Science and Engineering, Carnegie Mellon University,
Pittsburgh, Pennsylvania*

J. O. Cross and V. G. Harris
Naval Research Laboratory, Washington, DC

C. Franchetti
Department of Mathematics, University of Pennsylvania, Philadelphia, Pennsylvania

A new class of nanocrystalline alloys with composition Fe₄₄Co₄₄Zr₇B₄Cu₁ has been developed. This and similar alloys of general composition (Fe, Co)-M-B-Cu (where M=Zr, Hf, Nb, etc.) have been named HITPERM. They offer large magnetic inductions and excellent soft magnetic properties at elevated temperatures. Thermomagnetic properties, permeability, and frequency dependent losses are described in this report. These alloys exhibit high magnetization that persists to the $\alpha \rightarrow \gamma$ phase transformation at 980 °C. Alternating current permeability experiments reveal a high permeability at 2 kHz with a loss value of 1 W/g at $B_s = 10$ kG and $f = 10$ kHz. © 1999 American Institute of Physics. [S0021-8979(99)52908-3]

I. INTRODUCTION

The development of magnets for high temperature power applications requires new bulk soft magnetic materials that (1) are capable of operating at higher temperatures and (2) possess higher combined inductions and permeabilities. Continued development of soft magnetic materials for high temperature magnetic applications (such as rotors in electric aircraft) will be greatly influenced by changes in the field of soft magnetic materials. In nanocrystalline materials, where the grains are much smaller than the exchange coherence length, the magnetic anisotropy is averaged over many grains and orientations.¹ Thus these nanocrystalline alloys may have coercivity that can be significantly reduced and alternating current (ac) permeability increased as compared with conventional alloys.

Recently nanocrystalline Fe-Si-B-Nb-Cu alloys and nanocrystalline Fe-M-B-Cu (M=Zr, Nb, Hf, etc.) alloys have been optimized to achieve small magnetostrictive coefficients and concomitant large permeabilities. Of these alloys, nanocrystalline soft magnetic materials based on Fe-Si-B-Nb-Cu and Fe-M-B-Cu have been patented under the tradenames FINEMETS² and NANOPERM,^{3,4} respectively. In FINEMETS, α -Fe₃Si nanocrystalline grains, with a D0₃ crystal structure, are observed. In NANOPERM, α -Fe nanocrystals with body-centered-cubic (bcc) (A2) structure are formed.

We have investigated (Fe, Co)-Zr-B-Cu produced by rapid solidification processing followed by primary crystallization. These and similar alloys with the composition (Fe, Co)-M-B-Cu, where M=Zr, Nb, Hf, etc., we call HITPERM.⁵ In the HITPERM alloys, nanocrystalline α' -FeCo grains (B2 structure) are formed exhibiting significantly improved high temperature magnetic properties than in the former two systems. HITPERM maintains large induc-

tions to high temperatures. In this work, synthesis, crystal structure, and magnetic properties of (Fe, Co)₈₈Zr₇B₄Cu alloys are used to support these alloys as excellent candidates for high temperature soft magnetic materials.

II. EXPERIMENTAL PROCEDURES

Samples of the composition Fe₄₄Co₄₄Zr₇B₄Cu₁ were prepared by arc melting of high purity electrolytic Fe, Co, Zr, Cu, and Fe₃B (90.75% metals basis) in an argon atmosphere. Amorphous ribbons were produced from the ingots using a single wheel melt spinning technique. The amorphous ribbons obtained from this process were 20–50 μ m in thickness. The ribbons were isothermally annealed (550 °C < T_{ann} < 750 °C) in an argon atmosphere for 1 h followed by water quenching. Differential thermal analysis (DTA) was used to examine the crystallization temperatures of an as-cast ribbon. A scanning rate of 0.167 °C/s was used for temperatures between 400 and 1200 °C. The ribbons were examined by x-ray diffraction (XRD) using a Scintag XDS 2000 diffractometer and Cu $K\alpha$ radiation. Synchrotron x-ray diffraction experiments were performed at the National Synchrotron Light Source to identify the superlattice reflections which are signatures of the ordered α' -FeCo phase. The energy of the x rays was 7112 eV ($\lambda = 1.748$ Å) and chosen to take advantage of the anomalous scattering of Fe near the Fe K edge.

A Lakeshore vibrating sample magnetometer (VSM) was used to measure the magnetization of the as-cast material from room temperature to 1000 °C, in a field of 500 Oe, and with a heating rate of 2 °C/min. A Walker Scientific alternating current (ac) permeameter was used to measure the room temperature permeability and coercivity with a field amplitude of 2.5 Oe. The as-spun ribbons were prepared for permeability measurement by winding them into laminated toroids followed by the standard isothermal anneal for nanocrystallization prior to measurement of ac properties.

^{a)}Electronic mail: dupre@elmap.e.rug.ac.be

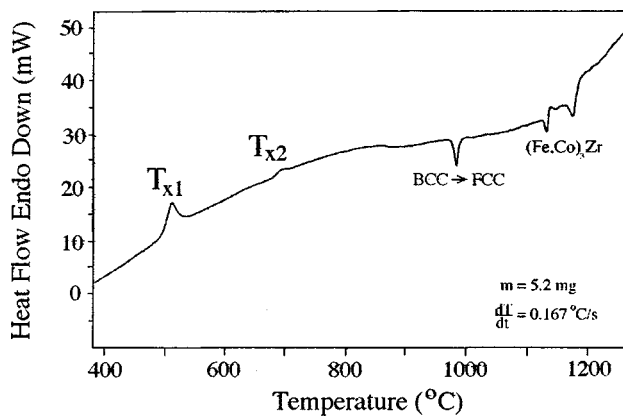
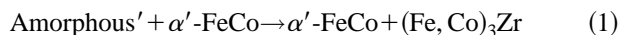
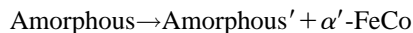


FIG. 1. Differential thermal analysis showing two distinct crystallization peaks, at $T_{x1}=510^\circ\text{C}$ and $T_{x2}=700^\circ\text{C}$. These peaks correspond to the crystallization of α' -FeCo and $(\text{Fe, Co})_3\text{Zr}$, respectively.

III. RESULTS AND DISCUSSION

Our alloy design was aimed at producing a stable α - or α' -FeCo phase after nanocrystallization that would provide the high saturation induction and Curie temperature. The addition of Zr and B were required for glass formation in the precursor alloy. Cu additions have been found to depress T_{x1} ,^{6,7} and are thought to provide nucleation sites for primary crystallization. DTA was used to determine the temperatures of crystallization for this alloy, as seen in Fig. 1. The reaction sequence:



seems to be the case for the crystallization at T_{x1} and T_{x2} , respectively. The primary and secondary crystallization temperatures occur at $T_{x1}=510^\circ\text{C}$ and $T_{x2}=700^\circ\text{C}$, for α' -FeCo and $(\text{Fe, Co})_3\text{Zr}$, respectively. The two distinct crystallization events allow the ferromagnetic α' -FeCo phase to form without the crystallization of nonferromagnetic phases which can degrade soft magnetic properties.

Conventional XRD results show the as-spun ribbon is amorphous, and the formation of either the α -FeCo or α' -FeCo phases occurs at annealing temperatures above T_{x1} . Inspection of the sample annealed at 750°C , just above T_{x2} , shows the formation of a small amount of $(\text{Fe, Co})_3\text{Zr}$ phase. Due to the similarity of the atomic scattering factors of Fe and Co, the observation of the superlattice reflections in conventional XRD is quite difficult. The ambiguity between the α - and α' -FeCo phases is removed by using the intense beam of a synchrotron x-ray source and choosing an x-ray energy to take advantage of anomalous scattering. The difference in atomic scattering factors were maximized by this choice of energy. In Fig. 2, the synchrotron XRD pattern shows that the atomically ordered α' -FeCo phase has indeed been formed by the presence of the (100) superlattice reflection. This sample was annealed at 550°C where we should expect the ordered phase.

Thermomagnetic data for amorphous alloys with the compositions $\text{Fe}_{88}\text{Zr}_7\text{B}_4\text{Cu}_1$ (NANOPERM) and $\text{Fe}_{44}\text{Co}_{44}\text{Zr}_7\text{B}_4\text{Cu}_1$ (HITPERM) were used to monitor crys-

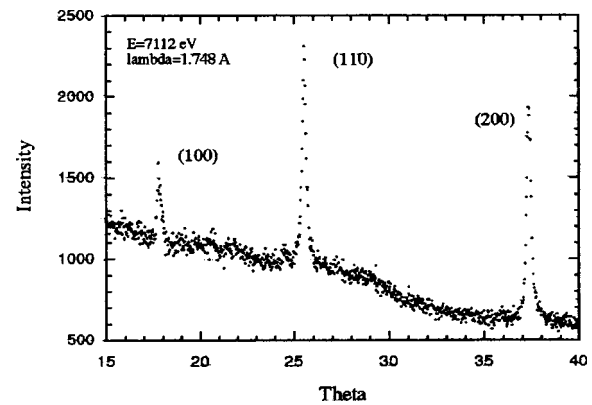


FIG. 2. Synchrotron x-ray diffraction experiment showing a (100) superlattice reflection, identifying the ordered α' -FeCo phase.

tallization events and to determine Curie temperatures. The Curie temperature of the NANOPERM amorphous alloy was just above room temperature, primary crystallization at $T_{x1} \sim 500^\circ\text{C}$, secondary crystallization at $T_{x2} \sim 700^\circ\text{C}$ and the Curie temperature for the α -Fe phase nanocrystals at $\sim 770^\circ\text{C}$. HITPERM alloys exhibited a monotonically decreasing magnetization as the amorphous phase approaches its Curie temperature. Above $\sim 500^\circ\text{C}$ crystallization of the α' -FeCo phase occurs resulting in a larger magnetization due to the higher Curie temperature of the α' -FeCo phase. The crystallization temperature is apparently well below the Curie temperature of the amorphous phase, so that the magnetization of the amorphous phase is only partially suppressed prior to crystallization. At the $\alpha \rightarrow \gamma$ phase transition temperature (980°C), the material abruptly loses its magnetization consistent with the paramagnetic response of the γ phase.

The ac magnetic hysteresis curves exhibited Rayleigh loop⁸ behavior for maximum fields less than the ac coercivity as illustrated in Fig. 3. Since the loops are sheared, they will not saturate at such a low field amplitude. With the low coercivity up to high frequencies, these materials show great promise if the process is properly optimized.

Low field amplitude ($H_m=2.5$ Oe) hysteresis loops have been measured at ac frequencies of 0.06, 4, 10, and 40 kHz, respectively. These are reasonably well fit by using a Raleigh

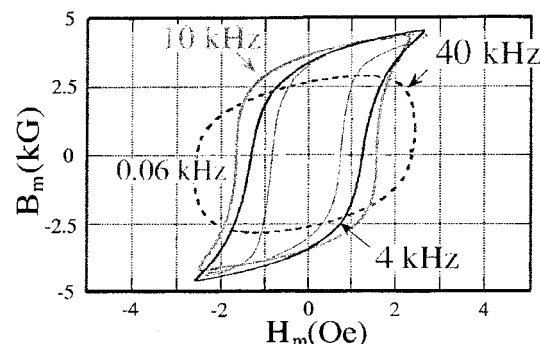


FIG. 3. ac hysteresis loops for the HITPERM alloy at 0.06, 4, 10, and 40 kHz. The sample was annealed at 600°C for 1 h and the measurements were made at room temperature with a field amplitude, $H_m=2.5$ Oe.

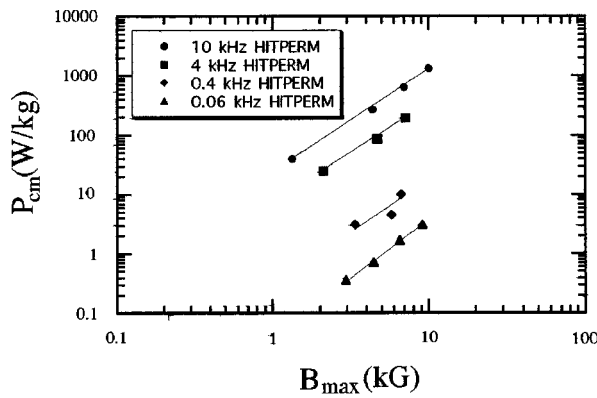


FIG. 4. Core loss for the HITPERM alloy annealed at 600 °C for 1 h. All experiments were run with a maximum field amplitude, $H_m = 2.5$ Oe at room temperature.

loop model, with the phenomenological hysteresis response as:

$$B \pm B_m = \mu_i(H \pm H_m) \pm v(H \pm H_m)^2,$$

where H_m is the ac field amplitude, B_m is the induction at H_m , μ_1 is the initial permeability, and $v = \partial\mu_i/\partial H$. The hysteretic contribution to the core loss increases as H_m^3 until saturation.

In Fig. 4, the core loss at various frequencies is plotted versus the maximum induction for the HITPERM alloy. These results are preliminary and are comparable to the room temperature results of Hiperco 50, a Carpenter Technologies alloy of nominal composition $Fe_{49}Co_{49}V_2$, which is currently used for high temperature applications. Field annealing of the nanocrystalline alloy will be helpful by shifting the curves to higher inductions. We believe the properly optimized HITPERM alloy will have better properties than its competitors at room temperature. At elevated temperatures, it will also have the advantage of better response due to the lowering of the magnetocrystalline anisotropy and magnetostrictive coefficients with increasing temperatures. Therefore, we should expect even better results for the HITPERM alloy at high temperatures up to 650 °C.

If we consider the complex permeability with $\mu = \mu' + i\mu''$, then we can plot the μ' and μ'' versus frequency as shown in Fig. 5. The μ' term as the real part of the permeability while the μ'' term as the loss term. At the frequency where μ' has an inflection and μ'' has a peak, we define a point called the cutoff frequency, which is ~ 2 kHz. In the HITPERM alloy, the maximum permeability was determined to be about 1800. The μ' permeability values are competitive with those of the Hiperco-50 alloy currently used for

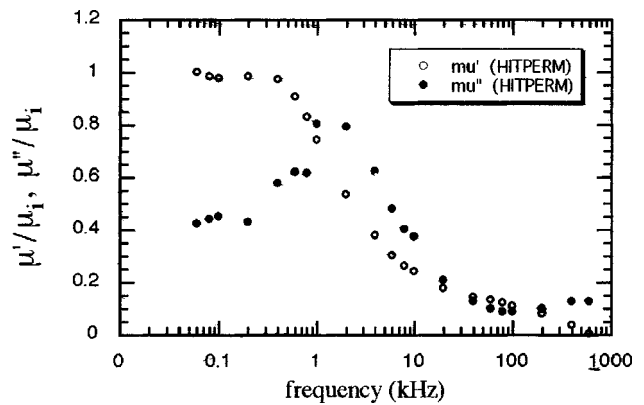


FIG. 5. ac permeability is shown as a function of frequency. The sample was prepared as a laminated toroid, annealed at 600 °C and measured with a field amplitude of 2.5 Oe at room temperature.

high temperature ac applications. The larger resistivity ($\rho = 50 \mu\Omega$ cm at 300 K) extends the large permeability to higher frequencies where eddy currents dominate the losses. The resistivity of the nanocrystalline materials is intermediate between the amorphous precursor and crystalline materials of similar composition.

ACKNOWLEDGMENTS

Effort sponsored by the Air Force Office of Scientific Research, Air Force Materiel Command, USAF, under Grant No. F49620-96-1-0454. The U.S. Government is authorized to reproduce and distribute reprints for Governmental purposes notwithstanding any copyright notation thereon. Work carried out in part at the National Synchrotron Light Source, Brookhaven National Laboratory, which is supported by the U.S. DOE. Special thanks to Johnny Kirkland for his help. Work carried out in part at Los Alamos National Laboratory, which is supported by the U.S. Department of Energy. DEL acknowledges partial support from NEDO project.

- ¹G. Herzer, IEEE Trans. Magn. **26**, 1397 (1990); G. Herzer, J. Magn. Magn. Mater. **112**, 258 (1992).
- ²Y. Yoshizawa, S. Oguma, and K. Yamauchi, J. Appl. Phys. **64**, 6044 (1988).
- ³K. Suzuki, A. Makino, N. Kataoka, A. Inoue, and T. Masumoto, Mater. Trans., JIM **32**, 93 (1991).
- ⁴A. Makino, T. Hatanai, Y. Naitoh, T. Bitoh, A. Inoue, and T. Masumoto, IEEE Trans. Magn. **33**, 3793 (1997).
- ⁵M. A. Willard, D. E. Laughlin, M. E. McHenry, D. Thoma, K. Sickafus, J. O. Cross, and V. G. Harris, J. Appl. Phys. **84**, 6773 (1998).
- ⁶K. Suzuki, A. Makino, A. Inoue, and T. Masumoto, J. Appl. Phys. **70**, 6232 (1991).
- ⁷A. Makino, A. Inoue, and T. Masumoto, Mater. Trans., JIM **36**, 924 (1995).
- ⁸Lord Raleigh, Philos. Mag. **23**, 225 (1887).